ELSEVIER

Journal of Nuclear Materials 312 (2003) 50–66

journal of nuclear materials

www.elsevier.com/locate/jnucmat

Thermodynamic properties of the O–U system. II – Critical assessment of the stability and composition range of the oxides UO_{2+x}, U_4O_{9-y} and U_3O_{8-z}

D. Labroche [a], O. Dugne [a], C. Chatillon [b,*]

[a] *Commissariat à l'Energie Atomique, VALRHO, DTE/STME, BP. 111, 26702 Pierrelatte, France*

[b] *Laboratoire de Thermodynamique et Physico-Chimie Métallurgiques (INPG/UJF/CNRS UMR 5614), ENSEEG, BP. 75, 38402 Saint Martin d'Hères, France*

Received 10 September 2001; accepted 14 October 2002

Abstract

The published data concerned with the determination of the composition ranges of uranium oxides, UO_{2+x}, U_4O_{9-y} and U_3O_{8-z}, which have been determined using thermogravimetric, X-ray diffraction and electrochemical techniques are critically assessed. U_4O_9 and U_3O_8 have quite small domains of composition and the assessment of such data has carefully considered the uncertainties in the experimental determinations. In addition, the thermodynamic properties of U_4O_9 and U_3O_8, enthalpies of formation and transformation, entropies, and thermal capacities are analyzed and selected to build a primary data base for compounds.

1. Introduction

The thermodynamic description of oxygen rich phases in the UO_2–UO_3 composition range of the O–U system that requires a base of critically evaluated thermodynamic data before any optimisation procedures [1] can be used to describe a self-consistent phase diagram. The previous analysis of chemical potentials of oxygen for the UO_2–U_3O_8 region of the phase diagram [2,3] is thus completed by this study which presents an analysis of the stability of the oxides, as well as a selection of data for their non-stoichiometric domains. A choice of reliable data in conjunction with an analysis of their related uncertainties will allow the optimisation of the O–U system, which takes into account the non-stoichiometric character of these oxides. One of the major aims of this study is the provision of a description of equilibria of the uranium oxides with other oxides. Particular applications would be in the fabrication of nuclear fuels with additions and behaviour of fuels under irradiation in a nuclear power plant.

In the analysis of the consequences of severe accidents in nuclear power plants a thorough knowledge of the high temperature behaviour of multicomponent systems is required. For the analysis of a PWR accident an understanding of the complex U–Zr–O system with the domains of non-stoichiometry is required; the effects of different atmospheres on the compositions and vaporisation behaviour at high temperatures must be understood.

The phase diagram and thermodynamic data optimisation procedure [1] is based on original data treated as a generalized least square fit, using the Gauss–Newton method in which each data *point* is weighted by the inverse of its uncertainty. Consequently, an important prerequisite is a careful evaluation of such uncertainties. As in the first paper of this series [2], the challenge is to analyse the uncertainties as close as possible to their real values, to compare different studies within their uncertainty limits when applying the law of propagation of

* Corresponding author.
E-mail address: chatillo@ltpcm.inpg.fr (C. Chatillon).

0022-3115/03/$ - see front matter
PII: S0022-3115(02)01323-5

errors [2–4] and finally *to* use our present knowledge of the O–U chemistry to select data when some are differing significantly within their assigned uncertainties.

2. The UO_{2+x}–U_4O_9 domain: the oxygen rich limit of UO_{2+x}

Techniques and methods for phase limit determinations are presented in Table 1, together with the retained uncertainties – either those proposed by the authors or more generally our estimates – for temperature and composition.

All these data are displayed in Fig. 1, and we observe general agreement between the different results and the shape of the phase limit is rather complex. We observe also some anomalous behaviour in the 1250–1350 K range, as well as two breaks, one at 800–850 K and another at 1400 K, which are due to phase transitions in U_4O_9, as discussed later since no transition is known for the UO_{2+x} phase.

As the phase limits obtained by EMF techniques have been discussed in the first paper, we shall mainly discuss those obtained by other techniques here.

2.1. Gronvold [11] XRD data

The phase limit was obtained by the intersection of the curves for lattice parameter values in the monophasic and diphasic domains for constant compositions

Table 1
UO_{2+x} upper oxygen phase boundary determinations according to literature

Authors	Sample	O/U measurement and uncertainty	Experimental technique, temperature uncertainty (K)
Kiukkola [5]	UO_{2+x}	Gravimetry: oxidation under air, 800 °C, $\delta x = \pm 0.01$	e.m.f., $\delta T = \pm 7$
Markin and Bones [6]	UO_{2+x}	Gravimetry: air oxidation, 800–900 °C, $\delta x = \pm 0.006$	e.m.f., $\delta T = \pm 7$
Saito [7]	UO_{2+x}	Gravimetry: air oxidation, 800 °C, $\delta x = 0.003$	e.m.f., $\delta T = \pm 7$
Marchidan et al. [8–10]	UO_{2+x}	Gravimetry: air oxidation, 800–900 °C, $\delta x = \pm 0.01$	e.m.f., $\delta T = \pm 7$
Gronvold [11]	UO_{2+x} and U_3O_8	From $UO_2 + U_3O_8$ original mixtures. No a posteriori check, $\delta x = \pm 0.01$[a]	XRD in a capillary tube (quartz) $a° = f(T, O/U)$, $\delta T = \pm 10$
Schaner [12]	UO_2 oxidized by $Ar + O_2$ or O_2 into UO_{2+x}	Gravimetry and chemical analysis, $\delta x = \pm 0.01$[a]	XRD on quenched samples at different speeds, $\delta T = \pm 10$
Aronson et al. [13]	UO_2 same as Schaner	$\delta x = \pm 0.01$	Conductivity, break in the slope, $\delta T = \pm 15$
Anthony et al. [14]	U_3O_8 reduction and quenching	Thermogravimetry by reduction into UO_2 under H_2 at $T = 1000$ K, $\delta x = \pm 0.01$	XRD on water quenched samples, $\delta T = \pm 5$
Kotlar et al. [15]	$UO_{2+x} \Longleftrightarrow U_3O_8$ by oxidation/reduction	Thermogravimetry at 800 °C, under air, $\delta x = \pm 0.00035$	Thermogravimetry, $\delta T = \pm 2$
Hagemark and Broli [16]	UO_{2+x}	Thermogravimetry at 800 °C, $\delta x = \pm 0.00007$	Thermogravimetry, $\delta T = \pm 5$
Kotlar et al. [17]	$UO_{2+x} \Longleftrightarrow U_3O_8$ by oxidation/reduction	Thermogravimetry at 800 °C under air, vaporization (UO_3) correction, $\delta x = \pm 0.0015$	Thermogravimetry, $\delta T = \pm 2$
Kotlar et al. [18]	$UO_{2+x} \Longleftrightarrow U_3O_8$ by oxidation/reduction	Gravimetry at 850 °C, under air, $\delta x = \pm 0.0012$	Thermogravimetry under temperature gradient for isopiestic transport, $\delta T = \pm 5$[a]
Blackburn [19]	UO_{2+x} by oxidation/reduction	Thermogravimetry with two references: UO_2 reduction H_2 at 1000 °C and U_3O_8 at 800 °C under 0.2 bar O_2, $\delta x = \pm 0.007$ (our estimate)	Knudsen method by weight loss, pressure measurements, $\delta T = \pm 5$[a]
Roberts and Walter [20]	UO_{2+x}	Continuous gravimetry by gain of O_2 (volumetry), $\delta x = \pm 0.002$	McLeod gauge total pressure measurements, $\delta T = \pm 5$
Picard and Gerdanian [21]	$UO_{2+x} \Longleftrightarrow U_3O_8$	Controled oxidation by gas volumetry, $\delta x = \pm 0.0003$	Calorimetry, $\delta T = \pm 2$

[a] Our estimate.

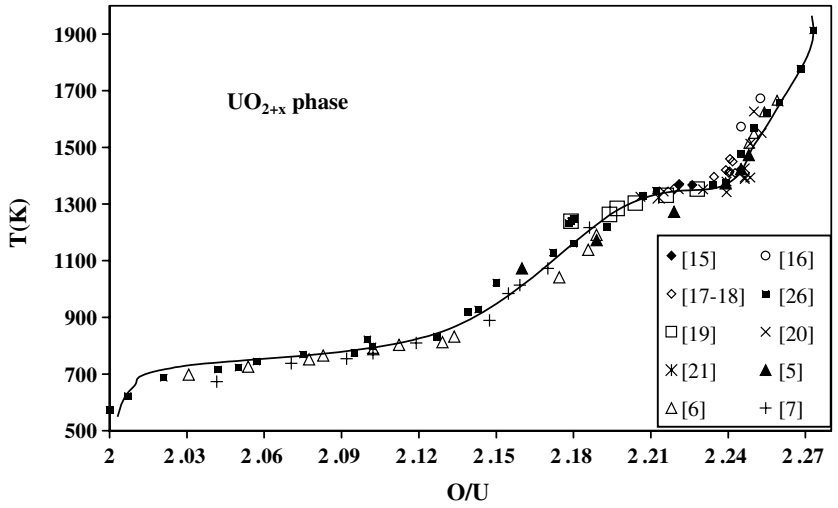

Fig. 1. Experimental phase diagram data for the upper oxygen phase boundary *limit* of UO_{2+x}.

as a function of temperature. At 1123 K and for $O/U = 2.15$, the quasi-parallel evolution of the two curves explains the large discrepancy observed for this data that we discard.

2.2. Schaner [12] data

Quenched samples were analyzed by ceramography and the phase limit is located between the last temperature for monophasic domain observation and the first temperature for appearance of the diphasic domain. The need for a sufficient quantity of the second phase to be observed explains the large temperature uncertainty, the resolution of the method being totally reported on the temperature.

For composition uncertainty, the author chose a UO_2 sample under pure H_2 gas in the 2018–2073 K range, with $O/U = 2 \pm 0.01$. In principle, UO_2 vaporizes non-congruently with effective loss of oxygen and its composition tends to become congruent [22,23], that is slightly hypostoichiometric ($O/U = 1.997$ at 2050 K). This tendency should be more pronounced under really pure H_2. However, as the published results of Schaner do not show any pronounced shift towards pure U when compared to other determinations, we believe that small oxygen or H_2O impurities allow the UO_2 reference composition to be really close to stoichiometry, within ± 0.01 as proposed by Schaner (50 ppm H_2O correspond to $p_{O_2} = 2.10^{-11}$ Pa for $O/U = 2$ according to Pattoret [22]).

Finally, the Schaner results, within their uncertainty range limits, confirm other determinations, but are not retained for the optimization procedure due to their too large temperature uncertainties and consequently too small and non-significant weighting.

2.3. Aronson et al. [13] electrical conductivity data

Aronson et al. measured the evolution of the electrical conductivity of pellets obtained from the experiments of Schaner [12]. Results agree with Shaner data [12] for $T < 1123$ K, but disagree at high temperature by 50 K or $\delta(O/U) = 0.02$. We believe that some impact of the environment (atmosphere, leak of gaseous contamination, chemical compatibility with electrodes, etc.) is the cause of these high temperature discrepancies with Shaner data and we discard these two high temperature data.

2.4. Blackburn [19] effusion data

Using the effusion method and following the weight loss by continuous weighing of an initial U_3O_8 sample due to $O_2(g)$ effusion, Blackburn observed breaks in $O_2(g)$ pressures at constant temperature that correspond to changes between diphasic and monophasic domains. Two main features have been discussed in the first paper [2]: (i) the existence of $UO_3(g)$ vaporization, (ii) the reference U_3O_8 composition obtained by calcination at 1073 K under O_2 pressure (0.2 atm in a thermobalance).

As discussed in the first paper, and according to Ackermann and Chang data [24], the U_3O_8 reference is in fact U_3O_{8-z} (with $\delta x(O/U) = -0.0105$ at 1073 K) when measuring the weight gain in a continuous and isothermal run with the thermobalance without any further temperature decrease under oxygen to recover the U_3O_8 composition as observed by Gerdanian and Dodé [25]. In addition, Blackburn used the UO_2–U_3O_8 composition range, based on a second reference UO_2 (H_2 at 1273 K in situ), to check the mass loss scale, and found correct results to within 0.25%, that is an uncertainty $\delta x = \pm 0.007$. This total uncertainty may corre-

spond roughly to the shift U_3O_8–U_3O_{8-z} as calculated according to Ackermann and Chang [24].

The second feature is the assumption of $O_2(g)$ being the lone species in the gas phase. The vaporization of $UO_3(g)$, as calculated in the first paper [2], leads to an overestimate of the mass loss and of the relative proportion of oxygen in this mass loss. The impact of $UO_3(g)$ on the U_4O_{9-y} and UO_{2+x} phase limits has been calculated in this first paper [2] (Table 6), and corrections may be done (an increase of x) leading to a phase limit more consistent with other data in the 1200–1400 K range as shown in Fig. 2. Applying the two corrections, $\delta x < 0$ from Ackermann and Chang corrections, and $\delta x > 0$ for $UO_3(g)$ vaporization, let Blackburn's values coming close to the original published values, but we have to take into account of these corrections in the assigned uncertainty. Thus we use the law of propagation of errors, $\delta x = (\delta x^2\ (\text{original}) + \delta x^2\ (\text{Ackermann corrections}) + \delta x^2\ (UO_3\ \text{vaporization}))^{1/2}$.

2.5. Kotlar et al. [17,18] data

In a first thermogravimetric study [17], the authors observed results in disagreement with those of Roberts and Walter [20]. In order to improve their method, thermogravimetric measurements were performed under isopiestic conditions to better control the gas transfer into or out of the sample [18]. Their earlier measurements were confirmed meanwhile the accuracy of the second set was improved for different reasons:

- the searched composition limit was necessarily reached, under isopiestic conditions generated by a temperature gradient and not bracketed as in the usual and isothermal method,
- the duration of the experiments was shortened, a feature that improved the stability of the thermobalance,
- and, as a consequence, corrections for $UO_3(g)$ vaporization became negligible.

Thus, we retain the second set of values [18], and the first one [17] only for the low temperature range where no other data were available, meanwhile the $UO_3(g)$ vaporization remained negligible.

In addition, we observe that Kotlar et al. data appear systematically richer in uranium than those of Roberts and Walters (Fig. 3) by $\delta(O/U) \leqslant 0.01$, neglecting the temperature uncertainty effects. As already proposed in the first paper [2], we believe this difference is due to nitrogen which is dissolved in the UO_{2+x} lattice since Kotlar et al. used $N_2 + O_2$ mixtures, and Roberts and Walter [20] pure O_2. However, as the uncertainties of these two sets overlap, we retain the two sets.

2.6. Conclusion for the UO_{2+x} limit

If Schaner's and Aronson data which are too inaccurate, the highest temperature data of Gronvold, a part of the Kotlar et al. first set are discarded, then the retained final data set is quite consistent. We then observe for this phase limit:

- that the oxygen solubility increases with temperature,
- that two breaks occur, one at 1400 K corresponding to the U_4O_9 peritectic decomposition into $U_3O_8 + UO_{2+x}$, and a second at 800 K which might correspond to a transformation of U_4O_9, since no transitions have been detected in the UO_{2+x} phase.

3. The U_4O_{9-y} non-stoichiometric compound

Until 1968 [25], those studying the properties of this compound assumed it was stoichiometric. Nevertheless,

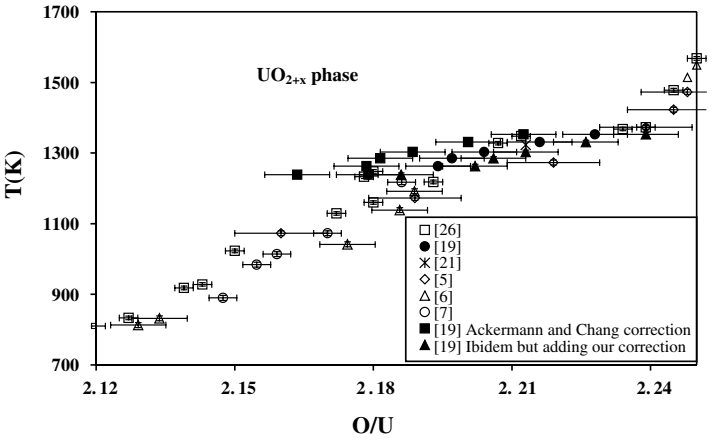

Fig. 2. Experimental phase diagram data reported with estimated uncertainties in the 800–1600 K range for the upper oxygen phase boundary of UO_{2+x}.

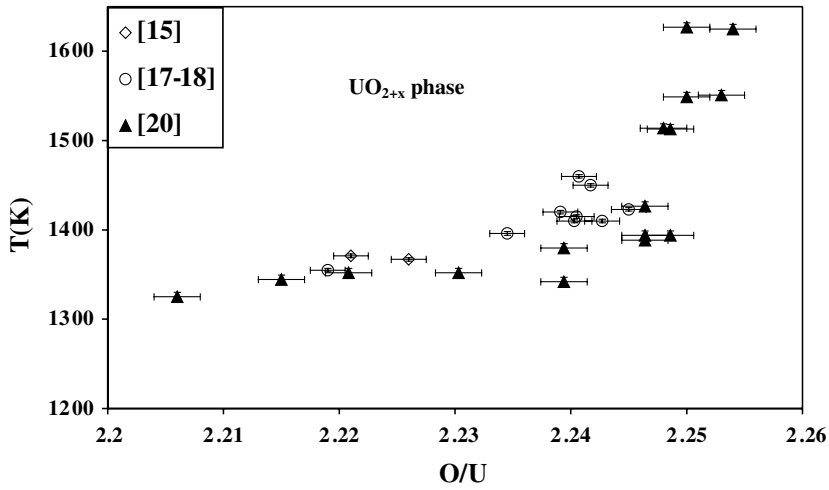

Fig. 3. Comparison of experimental phase diagram data, including the uncertainties, for the UO_{2+x} upper oxygen phase boundary limit obtained with a pure O_2 atmosphere by Roberts and Walter [20] and with a mixture $N_2 + O_2$ by Kotlar et al. [15,16,18].

potentiometric studies showed evolutions of oxygen chemical potential that corresponds to a non-stoichiometric domain and its composition range was tentatively determined as presented in Table 2 and Fig. 4. The scatter of the data appears as large as the non-stoichiometric domain, which thus needs a careful selection of these data in view of optimization.

3.1. The U_4O_{9-y} phase limits

3.1.1. Blackburn effusion data [19]

Same analysis as for the UO_{2+x} phase limit, and consequently the limits are corrected using the Ackermann and Chang correction and for $UO_3(g)$ vaporization, getting Blackburn data consistent with other authors, at least for the lower oxygen content phase boundary. For the higher oxygen content phase boundary, Blackburn observed a large round shaped pressure curve at the phase limit in place of a clear break, probably due to kinetic limitations in the effusion cell such as diffusion in the sample or surface phenomena as discussed in the first paper [2]. We discard these data because the boundary limit could not be determined with enough accuracy.

3.1.2. Schaner [12] and Van Lierde [27] data

Due to the technique used – samples quenched from a temperature plateau followed by ceramographic analysis – and the quasi vertical evolution of the lower oxygen phase boundary, Schaner's data are limited

Table 2
The U_4O_{9-y} phase limits as determined experimentally according to literature

Authors	Experimental technique	Temperature range and uncertainty δT (K)	Composition and uncertainty δ (O/U)
Van Lierde [27]	XRD, metallography electronic diffraction	1373 and 298, $\delta T = \pm 5$[a]	Chemical analysis, $\delta x = \pm 0.005$
Schaner [12]	XRD, metallography	1213 and 298, $\delta T = \pm 5$[a]	Gravimetry, $\delta x = \pm 0.01$
Picard and Gerdanian [21]	Calorimetry	$1323\delta T = \pm 5$[a],	Gaseous volumetry, $\delta x = \pm 0.0003$
Kotlar et al. [17]	Thermogravimetry	1355–1396, $\delta T = \pm 2$	Thermogravimetry, $\delta x = \pm 0.0015$
Roberts and Walter [20]	Thermogravimetry and McLeod gauge	1220–1750, $\delta T = \pm 5$[a], decomposition at $T = 1396$	Continuous gravimetry by gain of O_2 (volumetry), $\delta x = \pm 0.002$
Blackburn [19]	Effusion method in thermogravimetry	1230–1380, $\delta T = \pm 5$[a]	Thermogravimetry ref. U_3O_8 under O_2 (0.2 atm) at 800 °C, $\delta x = \pm 0.007$[a]
Gerdanian and Dodé [26]	Isopiestic method in thermogravimetry	1350–1380, $\delta T = \pm 5$[a]	Thermogravimetry ref. U_3O_8 slowly cooled to room temperature (1 atm $N_2 + O_2$), $\delta x = 0.0014$

[a] Our estimate.

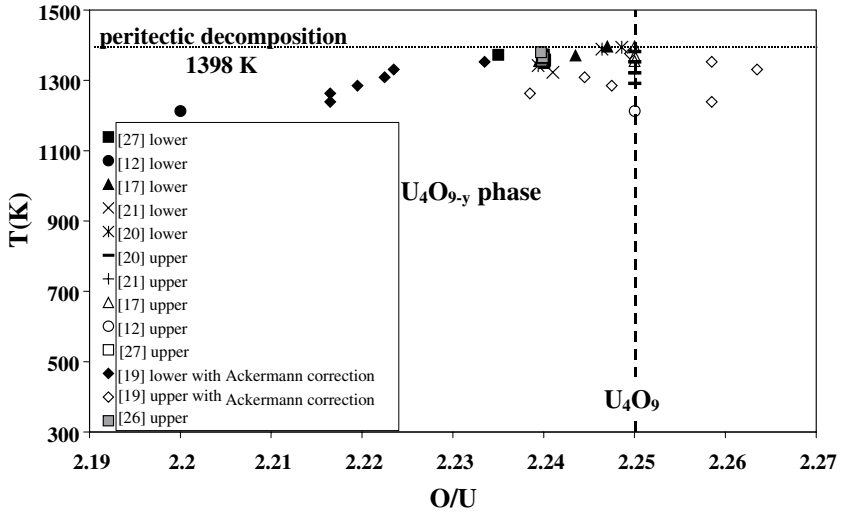

Fig. 4. Experimental phase diagram data for the non-stoichiometric domain U_4O_{9-y}. 'lower'-values for lower oxygen phase boundary, 'upper'-values for the U_4O_9 compound ($O/U \cong 2.25$).

and have large uncertainties. The author discussed the quenching efficiency of UO_{2+x} in ampoules, observing that for $O/U > 2.16$, and even for ampoules that were broken intentionally during the quenching process in water, the UO_{2+x} solutions could not retain the oxygen atoms and a two phases mixture was observed. Consequently, the quenching process is not effective and the phase boundary appeared shifted towards richer U compositions. The comparison with the results of other authors indicated that the above interpretation is correct (Fig. 4). Low oxygen boundary data of Schaner are thus discarded.

After careful examination of Schaner's results and technique, Van Lierde [27] explained that the ceramographic observation of phase limits suffers from large uncertainties. This is because the sample polishing and H_2O_2 attack, that precede the optical or electronic (SEM) microscopic observation, produce various UO_3(s) layers on UO_{2+x} and U_4O_9 compounds, the contrast of which is disturbed by crystal orientations. These features explain also the large difference between these two authors for the low oxygen phase limit although they applied the same method. Consequently the uncertainty limits are difficult to ascribe, and the only way forward is to check their consistency with other data. In the high temperature range, (1213 and 1373 K) we do not retain these values since other measurements are available.

3.1.3. Kotlar et al. [17], Gerdanian and Dodé [26], Picard and Gerdanian [21] data

These three studies on the same or related apparatus lead to upper and lower oxygen phase boundaries which are in agreement, and as shown in Fig. 4, their stoichiometric domain appears smaller than those of other authors. As these authors used $N_2 + O_2$ gas mixtures in their thermobalance, with a final calcination into U_3O_8 (in situ), an attempt has been made to evaluate the influence of nitrogen in the phase boundary determinations.

A compilation by Benz et al. [28] of the N–O–U system, obtained from X-ray diffraction and metallographic studies shows that solid solutions exist between UO_2–UN and UO_2–U_2N_3, with large solubilities in the 1873–2273 K range. On the isothermal section at 1273 K, the working temperature of Kotlar et al., Gerdanian and Dodé, and Picard and Gerdanian, a solid solution of U_2N_3 in UO_2 extends up to 10 at.% of N, and Benz et al. [28] propose a substitution of O^{2-} by N^{3-} based on the lattice parameter increase with N_2 pressure. The work of Benz et al. clearly shows that the N_2 gas is reactive and that some solubility of nitrogen in the lattices of U oxides may occur at least in the calcination stage with modification of the gravimetric reference composition U_3O_8. The influence of nitrogen is evaluated by the following calculations.

Starting from a mass m of UO_2 in g, the number of U atoms is $N_U = m/270$. The final U_4O_9 sample has the mass of $UO_{2.25}$: $M = m + \Delta m$. In case 1, only O is introduced in the lattice, and thus the O/U ratio is:

$$\left(\frac{O}{U}\right)_1 = \frac{2N_U + \frac{\Delta m}{16}}{N_U}.$$

In case 2, O and N (with the proportion x of final N) are introduced in the compound:

$$\left(\frac{O}{U}\right)_2 = \frac{2N_U + (1-x)N_T}{N_U}$$

with

$$N_T = \frac{\Delta m}{16(1-x)+14x},$$

and finally:

$$\left(\frac{O}{U}\right)_2 - \left(\frac{O}{U}\right)_1 = 270\frac{\Delta m}{m}\left(\frac{1-x}{16(1-x)+14x} - \frac{1}{16}\right).$$

For an initial sample of 1 g of UO_2, $\Delta m = 0.00148$ g, and the final compositions are calculated for different N proportions (Table 3). Results show correct agreement with the gap existing between Kotlar et al., Picard and Gerdanian and Gerdanian and Dodé and the other studies, Blackburn [19] Roberts and Walters [20], for a reasonable proportion of N dissolved in U_4O_9 and UO_{2+x} when comparing Table 3 and the original data in Fig. 3.

Thus, we believe that N_2 as a carrier gas has influenced the composition range limits of the two compounds UO_{2+x} and U_4O_9, explaining the shift towards U rich compositions of all authors using this gas as compared to other authors.

3.1.4. Conclusion

Observing the extend of the non-stoichiometric range of the U_4O_{9-y} compound as determined by potentiometric methods, we find that there is an acceptable agreement between the different studies [17,19–21,26], but they differ in scaling to the reference composition U_3O_{8-z}, which is probably due to the calcination process as discussed in the first paper [2] and to the presence of N_2 as a carrier gas.

In terms of absolute values for compositions of the phase limits, we thus retain the Roberts and Walters data [20] obtained under a pure O_2 atmosphere, and with an acceptable composition reference. However, we do not understand why the Picard and Gerdanian values [21] do not agree with this limit, since they worked with pure O_2(g) in this study. We simply quote that in their calorimetric measurements under volumetric titration, the authors observed some heterogeneous consumption of O_2(g) going in parallel with a decrease of the reaction kinetics in monophasic domains probably due to a diffusion or a surface transfer rate limited process. This feature may prevent or hide the attainment of the upper phase limit. For the lower oxygen phase boundary, in the absence of kinetic problems for measurements in the diphasic UO_{2+x}–U_4O_{9-y}, the Picard and Gerdanian [21] data agree with the Roberts and Walters [20] data as well as with those of Blackburn [19]. When scaling the Kotlar et al. data [17] on the upper oxygen limit of Roberts and Walters, we observe that the values for the lower limit agree, but we cannot arbitrarily move these data, since their is no thermodynamic reason for a constant nitrogen effect across the non-stoichiometric domain. Therefore, we do not retain these data (Fig. 5).

Table 3
Influence of small nitrogen content in the determination of phase limits of U_4O_9 by calcination into U_3O_8

N molar fraction (%)	O/U only O	O/U with O + N
0	2.25	–
1	–	2.248
5	–	2.239
10	–	2.228

In the low temperature range – i.e. room temperature – we observe that Inaba and Naito [29] have performed XRD measurements from O/U = 2.25 to 2.226, apparently in the non-stoichiometric domain, with a phase limit located at 2.228 that we retain. However, we propose to discard the data of Schaner and Van Lierde [12,27]. We shall further see that considerations on the structure and defects favour a low oxygen phase limit to be a vertical line in the low temperature range (one paper of this series) at the O/U = 2.23 composition. For the high oxygen concentration, according to Inaba and Naito [29] as well as Roberts and Walter [20], we retain a vertical limit at O/U = 2.25.

3.2. Phase transitions of U_4O_9

Gronvold [11] observed a lattice contraction between 239 and 359 K, meanwhile Westrum and Gronvold [30] proposed a phase transition at about 350 K on the basis of thermal capacity differences between 1/4 U_4O_9 and 1/3 U_3O_7. Belbeoch et al. [31], later confirmed by Gilardy [32], showed by electron diffraction that samples, the composition of which is in the range UO_2–U_4O_9, heat treated and quenched by different ways may be ordered or not. Then, different investigations were performed as summarized in Table 4, that show two phase transitions.

3.2.1. The low temperature transition (~350 K)

The agreement between authors is quite good as shown in Fig. 6, the transition temperature being decreasing slowly for compositions richer in oxygen. However, some scatter exists for O/U = 2.25 which can be explained:

- according to Naito et al. [34], the earlier Westrum et al. [41] measurements were performed with inaccurate composition control and on irradiated samples,
- inaccurate composition for Gronvold et al. [39],
- internal heating of the sample in the case of Gotoo and Naito [35] that leads to a lag time in the detection

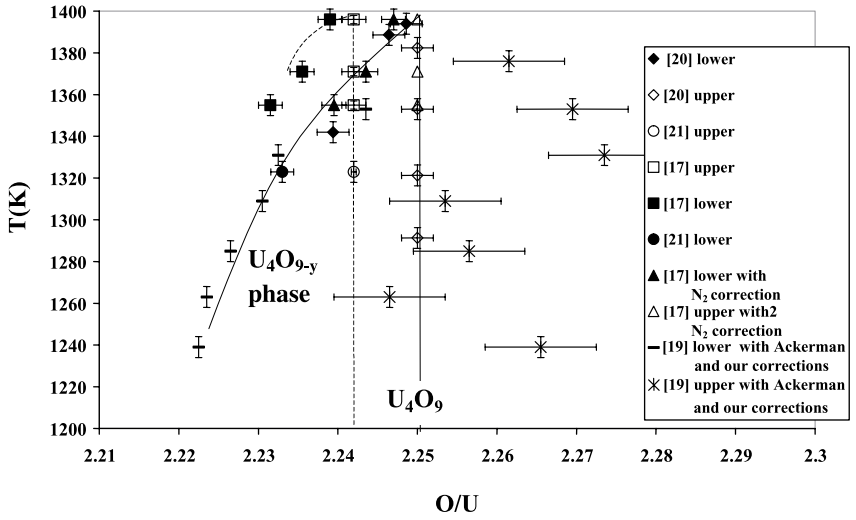

Fig. 5. Experimental phase diagram data obtained by EMF and partial pressure methods in the high temperature range close to the decomposition of the U_4O_9 phase. Corrections due to N_2 in the atmosphere as well as due to the U_3O_8 reference composition are discussed in the text.

of thermal effects, conversely to other determinations with external heating of the sample.

The nature of this transition has been discussed:

- Gotoo and Naito [35] discarded any magnetic transition since their specific heat C_p° results showed a paramagnetic effect up to 500 K, meanwhile theoretical considerations on susceptibility indicated a cation distribution between U^{4+} and U^{5+},
- Naito [42], from a XRD study and lattice contraction, noted an intensity increase of superstructure rays and proposed an anion rearrangement, but this one effect cannot explain the observed entropy increment at the transition,
- Naito [42], by comparison with Fe_3O_4 behavior and following the interpretation of Tateno [43], proposed finally an order–disorder phase transition, for which the ordered energy, the activation energy and the mid-transition temperature were successfully correlated with electrical conductivity measurements.

Thermodynamic properties obtained by adiabatic calorimetry and associated with this transition, mainly extrapolated to null scanning speed, are presented in Table 5. We observe that these properties vary with composition in the non-stoichiometric domain of U_4O_{9-y}. In order to confirm the mechanism of this transition – i.e. order–disorder transition with U^{4+}–U^{5+} rearrangement and valence electron configuration change, Naito et al. [34] and more successfully Inaba and Naito [29] recalculated the entropy contributions from electrical conductivity measurements that agree with calorimetric determinations.

3.2.2. The high temperature transition (≅850 K)

Blank and Ronchi [38] proposed from XRD analysis an order–disorder transition in the 823–973 K range, meanwhile Gronvold et al. [39] observed some anomaly on the C_p° evolution starting in the 900–950 K range. Naito et al. [34] using XRD and electrical conductivity proposed the same mechanism as for the low temperature transition in the 813–893 K range and for $2.228 \leqslant O/U \leqslant 2.25$. Seta et al. [36] recently observed an increase of thermal capacity as well as a lattice contraction by XRD. Differences in the proposed transition temperatures come probably from kinetic phenomena linked to the energy impulse method used by Seta et al. [36]. Conversely to the low temperature transition, its thermodynamic properties have not been calculated since no clear and marked C_p° variation (peak) have been observed, except a regular increase of the thermal capacity. It should also be noted that the drop calorimetry measurements of McLeod [44], were not sufficiently sensitive to reveal any anomaly in the 800–1600 K range, but show a small increase of C_p° with temperature.

The observation of a break in the UO_{2+x} upper oxygen phase boundary at 830 K could be, in the absence of phase transition for UO_{2+x}, ascribed to a transition for U_4O_{9-y} which is observed with XRD and electrical conductivity. This transition appears as a second order one, the thermodynamic properties of which are only revealed by an increase of the thermal capacity ($\Delta H_{tr} = \Delta S_{tr} = 0$).

Table 4
Transition temperatures determined for U_4O_9 and experimental techniques used

Authors	Experimental technique	Transition temperature (K) and uncertainty	Composition
Westrum et al. [41]	Adiabatic calorimetry	348 ± 5	$U_4O_9 \pm 0.01$[a]
Osborne et al. [33]	Adiabatic calorimetry	No transition for $5 < T < 310$	$U_4O_9 \pm 0.01$[a]
Naito et al. [34]	Electrical conductivity, XRD	350 ± 5[a]	$UO_{2.228} \pm 0.002$[b]
		345 ± 5	$UO_{2.24} \pm 0.002$
		335 ± 5	$UO_{2.25} \pm 0.002$
		833 ± 5	$UO_{2.228} \pm 0.002$
		853 ± 5	$UO_{2.24} \pm 0.002$
		893 ± 5	$UO_{2.25} \pm 0.002$
Inaba and Naito [29]	Adiabatic calorimetry	351 ± 5[a]	$UO_{2.246} \pm 0.002$[b]
		344 ± 5	$UO_{2.24} \pm 0.002$
		342 ± 5	$UO_{2.25} \pm 0.002$
Gotoo and Naito [35]	Conductivity	330 ± 5[a]	$UO_{2.246} \pm 0.01$[a]
Seta et al. [36]	Conductivity, thermal capacity	352 ± 5[a]	$UO_{2.22} \pm 0.002$[a]
		350 ± 5	$UO_{2.235} \pm 0.002$
		345 ± 5	$UO_{2.25} \pm 0.002$
		850 ± 5	$UO_{2.25} \pm 0.002$
		1027–1091	$UO_{2.235} \pm 0.002$
		1004–1110	$UO_{2.22} \pm 0.002$
Lauriat et al. [37]	Neutron diffraction, Scanning calorimetry	345 ± 3[b]	$UO_{2.25} \pm 0.005$[b]
Blank and Ronchi [38]	Electronic diffraction	At $T > 723$ change of structure $\delta T = \pm 40$[b]	$UO_{2.25} \pm 0.01$[a]
Gronvold et al. [39]	Adiabatic calorimetry	348 ± 5[a]	$UO_{2.254} \pm 0.003$[a]
		900 ± 5	$UO_{2.254} \pm 0.003$[a]
Ishii et al. [40]	XRD	348 ± 5[a]	$UO_{2.237} \pm 0.01$[a]
		337 ± 5	$UO_{2.248} \pm 0.01$

[a] Our estimate.
[b] Authors estimate.

3.2.3. Peritectic decomposition of U_4O_9

The different decomposition temperatures from the literature are presented in Table 6. The values of Kiukkola [5], Belbeoch et al. [45] and Matsui and Naito [47] seem largely scattered when compared to the ~1400 K value directly determined, probably because in some XRD experiments the temperature measurements were inaccurate. Saito [7] proposed an extrapolated value from EMF measurements which is 80 K higher than the average value, probably because the slope of EMF measurements may have some systematic error or trend. We propose to retain the mean value of Blackburn [19], McLeod [44], Dodé and Touzelin [46], Van Lierde [27] and Roberts and Walter [20]:

$$T(\text{peritectic dec.}) = 1397.8 \pm 8 \text{ K}.$$

The lone enthalpy of decomposition measured by McLeod [44] is retained,

$$\Delta H_{\text{tr}}(\text{peritectic}) = 11.9 \pm 0.1 \text{ kJ mol}^{-1}$$

in agreement with the Cordfunke and Konings [48] choice for the same reason: the proposed value by McLeod – because of a poorly explained mathematical treatment – is discarded.

3.3. Thermodynamic properties of the compound $U_4O_9(s)$

The formation enthalpy of $U_4O_9(s)$ has been measured by dissolution calorimetry in cerium solutions by Fitzgibbon et al. [49] and in nitric acid solution by Burdese and Abbatista [50]. The last and less accurate value confirms the first one which is retained as already proposed by Glushko et al. [51] and Cordfunke and Konings [48].

The high temperature thermal capacity has been measured by different techniques as summarized in

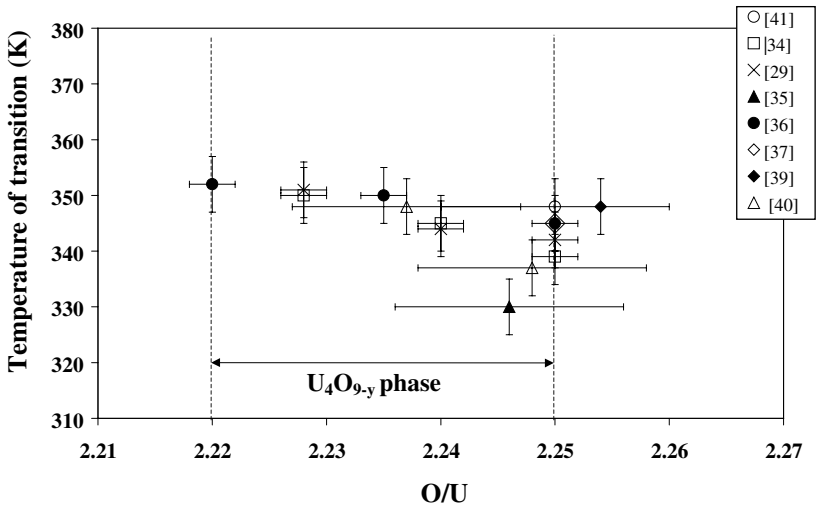

Fig. 6. Low temperature transition data for U_4O_{9-y} as a function of composition. A slight decrease is observed when the compound becomes richer with oxygen.

Table 5
Thermodynamic properties associated with the low temperature transition of U_4O_9 at 350 K

Authors	O/U	T (K) transition	ΔH° J mol^{-1}	ΔS° J K^{-1} mol^{-1}
Inaba and Naito [29]	2.228 ± 0.002	351 ± 5	987 ± 13	2.93 ± 0.04
	2.24 ± 0.002	344 ± 5	774 ± 13	2.34 ± 0.04
	2.25 ± 0.002	352 ± 5	632 ± 13	1.92 ± 0.04
Gotoo and Naito [35]	2.246 ± 0.01	330 ± 5	711 ± 21	2.09 ± 0.04
Westrum et al. [41]	2.25 ± 0.01	348 ± 5	628 ± 8	1.88 ± 0.04
Gronvold et al. [39]	2.254 ± 0.003	348 ± 5	690 ± 71	2.18 ± 0.21

Table 6
Peritectic transformation temperature of U_4O_9 into $UO_{2+x} + U_3O_8$ according to literature

Authors	Experimental technique	Peritectic temperature (K) and uncertainty
Blackburn [19]	Knudsen effusion method/thermobalance	1399
Roberts and Walter [20]	Vapour presure measurements	1396 ± 5
Kiukkola [5]	e.m.f.	1443
Belbeoch et al. [45]	X-ray diffraction	1373–1423
Van Lierde et al. [27]	Metallography	1398
Dodé and Touzelin [46]	X-ray diffraction	1398
Matsui and Naito [47]	Electrical conductivity	1423–1473
	X-ray diffraction	1399–1404
McLeod [44]	Drop calorimetry	1398 ± 8
Saito [7]	e.m.f.	1479 (extrapolated)

Table 7 and compared with preceding compilations in Fig. 7. Results generally agree but not for temperatures corresponding to the low transition temperature range (300–400 K), and only for $T < 830$ K. Thus, we retain the Cordfunke and Konings [48] or SGTE [54] least square fit in the 298–830 K range. At higher temperature and in order to take into account of the high temperature transition, we propose a new fit. All the retained thermodynamic properties of the U_4O_9(s) compound are summarized in Table 8.

Table 7
Thermal capacities according to literature. Original data for the compound U_4O_9(s)

Authors	Experimental technique	Temperature range (K)	Composition and uncertainty (%)	C_p° and uncertainty
Westrum et al. [41]	Adiabatic calorimetry	190–400, $\delta T = \pm 5$	U_4O_9, $\delta x = \pm 0.08$	$\delta C_p = \pm 0.1\%$, For $T > 25$ K, From [33]
Osbome et al. [33]	Adiabatic calorimetry	5–305, $\delta T = \pm 5$	U_4O_9, $\delta x = \pm 0.08$	$\delta C_p = \pm 0.1\%$, $T > 25$ K, $\delta C_p = \pm 1\%$ at 14 K, $\delta C_p = \pm 5\%$ at 5 K
Seta et al. [36]	Calorimetry with impulsional heating	300–1180, $\delta T = \pm 5$	$UO_{2.25}$, $UO_{2.235}$, $UO_{2.22}$, $\delta x = \pm 0.002$	$\delta C_p = \pm 1.5\%$, $T < 1000$ K, $\delta C_p = \pm 2.1\%$, $T > 1000$ K
Gronvold et al. [39]	Adiabatic calorimetry	300–1000, $\delta T = \pm 5$	$UO_{2.254}$, $\delta x = 0.001$	
Inaba and Naito [29]	Adiabatic calorimetry	180–470, $\delta T = \pm 5$	$UO_{2.25}$, $UO_{2.235}$, $UO_{2.22}$	$\delta C_p = \pm 2\%$
McLeod [44]	Drop calorimetry	845–1395		C_p° derived from enthalpy increments

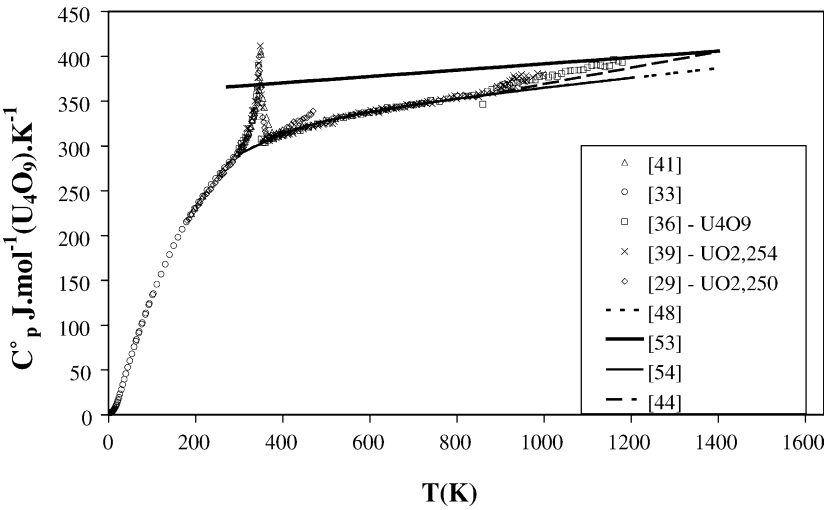

Fig. 7. Thermal capacity data of U_4O_9 from literature and comparison with proposed least square fits [44,53,54].

4. The U_3O_{8-z} non-stoichiometric compound

4.1. The U_3O_{8-z} phase limits

Experimental studies performed in order to determine the boundary limits of the U_3O_{8-z} non-stoichiometric compound are presented in Table 9. Some authors proposed the existence of new compounds U_3O_7 or U_8O_{21}, close to the U_3O_8 composition:

Caneiro [62] from thermogravimetric measurements proposes the existence of the U_8O_{21} compound. We rejected this interpretation on the basis of kinetic limitations in his measurements (see previous paper [2]): Caneiro observed an evolution of composition at a near constant pressure of O_2 when decreasing the O_2 partial pressure of the flow of gas, but he did not recover this pressure when increasing the O_2 partial pressure. The hysteresis behavior of the curves $\log p_{O_2} = f(O/U)$ clearly indicates non-reversible behavior that we attribute to two different kinetics for adsorption and desorption of oxygen in place of metastable phases proposed by the author [62]. The non-reversibility of the constant pressure plateau is a first indication of some kinetic effect in place of the sign of the creation of a second phase because when increasing again the pressure of O_2(g) the disappearance of the proposed second phase should show a plateau, even occurring at a different pressure value. Indeed, Blackburn [19] observed by mass spectrometry that the evaporation coefficient of O_2(g) in this composition range was lower than the value unity, showing that the O_2 desorption was kinetically hindered.

Table 8
Summary of proposed values for thermal properties of the stoichiometric U_4O_9(s) in this work

Thermodynamic quantity	Retained values	From reference
Enthalpy of formation	$\Delta H_f^\circ(U_4O_9, s, 298.15\ K) = -4512 \pm 7\ kJ\,mol^{-1}$	[48,49,51,54]
Entropy at 298 K	$S_{298}^\circ = 334.1 \pm 0.4\ J\,K^{-1}\ mol^{-1}$	[33,52,54]
Peritectic decomposition	$T = 1398.5 \pm 8$ K, $\Delta H_{dec} = 11900 \pm 100\ J\,mol^{-1}$	[44]
Low temperature transition	$T = 345 \pm 10$ K for O/U = 2.22 to $T = 335 \pm 10$ K for O/U = 2.25. $\Delta H_{tr} = 737 \pm 50\ J\,mol^{-1}$ et $\Delta H_{tr} = 631$ J/mol	[29,35,41,39]
High temperature transition	$T = 850 \pm 20$ K, $\Delta H_{tr} = 0$	[35,38]
Thermal capacity ($J\,K^{-1}\,mol^{-1}$)	$C_p^\circ = 319.163 + 0.049691T - 3960200/T^2$	$298 < T < 850$ K [48]
	$C_p^\circ = 281.5 + 88.836 \times 10^{-3}T - 1175737.6/T^2$	$850 < T < 1397.5$ K [44]

Table 9
Experimental studies on the phase limits of the U_3O_{8-z} non-stoichiometric compound according to literature

Authors	Experimental techniques and uncertainties	Compositions analysis (O/U = x) and uncertainties
Hoeckstra et al. [55]	XRD at high temperature in capillary tubing $\delta T = \pm 10$ K	Gravimetry/calcination 750 °C, Air; $\delta x = \pm 0.01$
Kotlar et al. [17]	Thermogravimetry ($N_2 + O_2$), $\delta T = \pm 2$ K, $\delta p_{O_2}/p_{O_2} = \pm 5\%$	Calcination ($N_2 + O_2$) 800 °C, Air; $\delta x = \pm 0.0015$
Blackburn [19]	Knudsen effusion/thermobalance, $\delta T = \pm 2$ K	Calcination in situ O_2 at 800 °C, $\delta x = \pm 0.007$
Ackermann and Chang [24]	Thermogravimetry (Ar + O_2), $\delta T = \pm 5$ K, $\delta p_{O_2}/p_{O_2} = \pm 13\%$	Calcination in situ, $\delta x = \pm 0.002$
Sata [56]	Thermogravimetry (Air, N_2, O_2), XRD and quenching in water or Hg, $\delta T = 5$ K	Gravimetry under H_2 at 750 °C (reduction), $\delta x = \pm 0.002$
Gronvold [11]	High temperature XRD, $\delta T = \pm 5$ K	Gravimetry under O_2 at 800 °C, $\delta x = \pm 0.01$
Caneiro and Abriata [57]	Thermogravimetry ($Ar + O_2$), $\delta T = \pm 5$ K, $\delta p_{O_2}/p_{O_2} = \pm 2\%$	Gravimetry by H_2 reduction at 1173 K, $\delta x = \pm 0.0002$
Ishii et al. [58]	Electrical conductivity under air, $\delta T = \pm 5$ K	Gravimetry by H_2 reduction at 1000 °C, $\delta x = \pm 0.01$
Matsui et al. [59,60]	Thermogravimetry ($Ar + O_2$) Electrical conductivity XRD at high temperature, $\delta T = \pm 5$ K, $\delta p_{O_2}/p_{O_2} = \pm 2.3\%$	Gravimetry by H_2 reduction at 1000 K, $\delta x = \pm 0.0002$
Kozhina and Shiryaeva [61]	High temperature XRD, $\delta T = \pm 10$ K	$\delta x = \pm 0.002$ proposed by the authors (No information)

Ishii et al. [58] observed an evolution of the electrical conductivity under atmospheric pressure above 800 K, that we attribute to a non-stoichiometric behavior on the basis of Ackermann and Chang [24] work. Indeed, and in agreement with Caneiro's observations, the electrical conductivity measurements were not reversible when cycling.

Hoeckstra et al. [55] by in situ and also after cooling XRD measurements, observed some modifications in the diffraction patterns that are also confirmed by Sata [56] and Ishii et al. [63], but that would be related to different superstructures as proposed by Kozhina and Shiryaeva [61]. Matsui et al. [59,60] observed six breaks in the slope of electrical conductivity measurements meanwhile one structure by XRD: the electrical conductivity would be only dependent on defects in relation with oxygen potential.

In an oxidation study of UO_2 in air, Hering and Pério [64] proposed the existence of the U_3O_7 compound, but in a later study, Pério [65] observed that after heat treating from low temperature (140 °C) to higher temperature (700 °C), this phase disappears and only U_4O_9 and U_3O_8 were identified at equilibrium. Gronvold [11] confirmed this feature. We conclude as Pério that the U_3O_7 is a metastable *compound and* this compound appears during oxidation probably because some mechanical constraints in the growth process stabilized this compound relative to the other oxides.

So, we conclude that the U_3O_7 and U_8O_{21} compounds are not stable ones or if they exist, they are metastable compounds, and the observed anomalies in the measurements are most probably related to kinetic phenomena.

The low oxygen phase boundary U_3O_{8-z}, has been determined by different techniques listed in Table 9 and presented in Fig. 8.

Gronvold [11] data are deduced from the evolution of the lattice parameter of constant composition samples contained in capillary tubings as a function of temperature. These measurements are not very accurate, but still remain useful for delimiting the low temperature domain: for this reason, we retain the room temperature measurement for the optimization procedure.

Other determinations are potentiometric and have been analyzed in the first paper [2]. We selected the Blackburn [19] and Ackermann and Chang [24] data and consequently their deduced phase limits are also in agreement as observed in Fig. 8. The main disagreement between these selected phase diagram data and those deduced by Kotlar et al. [17], Hagemark and Broli [16], Caneiro and Abriata [57] come from lack of equilibrium that leads to lower measured pressures as explained in the first paper [2]. Consequently, when calculating the phase limit by the intersection of O_2(g) pressure with the well-known pressure in the diphasic U_4O_9–U_3O_{8-z} – domain for which all the authors agree – lower pressures give higher oxygen content as shown in Fig. 9. This feature explains the shift of Caneiro and Abriata [57], Kotlar et al. [17] and Hagemark and Broli [16] values (see Fig. 8) from those of Blackburn [19] and Ackermann and Chang [24], which we retain. Besides, we have to quote that, contrary to the U_4O_9 compound, working under N_2 carrier gas by Kotlar et al. [17] did not lead to clearly different results than under pure O_2(g) as carried

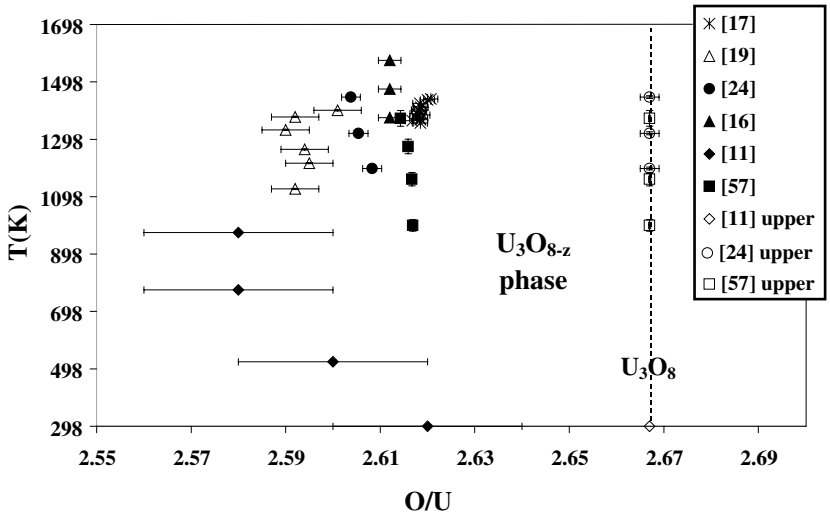

Fig. 8. Experimental phase diagram data with their estimated uncertainties for the non-stoichiometric domain of the U_3O_{8-z}.

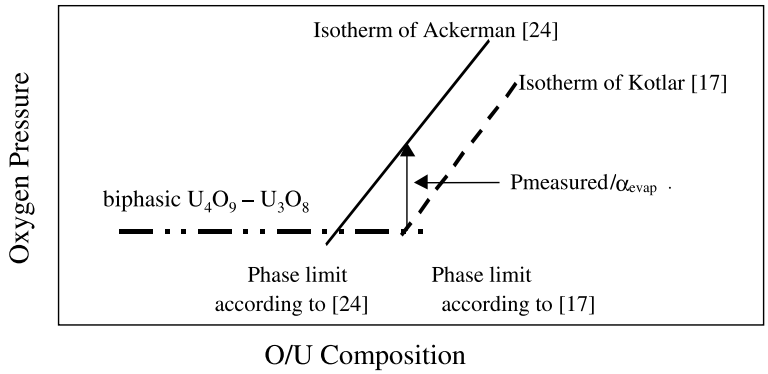

Fig. 9. Influence of lower pressures, as determined when kinetic limitations occur [17], on the phase limit determination according to [24]. The low oxygen limit is shifted toward richer oxygen compositions.

out by Hagemark and Broli [16]. Thus the influence of nitrogen seems less pronounced for the U_3O_8 than for the U_4O_9 compound.

The high oxygen boundary is chosen in agreement with all the authors as U_3O_8 or $UO_{(2+2/3)}$.

4.2. Phase transitions of U_3O_{8-z}

Four transitions have been detected by adiabatic scanning calorimetry (Table 10) and have been confirmed by other techniques: XRD [61,66], electrical conductivity [73] and dilatometry [55,74]. Some of these techniques, performed in order to control the composition or oxygen potential [61] or to obtain values extrapolated at null speed [72] confirm the calorimetric observations. Some authors [66–68,72] observed that the 2nd and 3rd transitions at about 490 and 570 K, showed a slight evolution of their transition temperature and enthalpy as a function of composition.

Electrical conductivity, dilatometry and XRD results have been interpreted in order to understand the nature of these transitions, in relation to changes in their thermal capacity evolutions. The dilatometric changes indicate that these transitions are not simple allotropic changes. From electrical conductivity measurements, Naito et al. [67] proposed an electronic ordering on cations with displacement of anions, the resulting b/a ratio of the orthorhombic structure moving towards the value $\sqrt{3}$, characteristic of an hexagonal structure.

The 850 K transition is less marked than the other transitions using adiabatic calorimetry, but is not observed with other techniques. For this reason, we believe this is probably an anomaly related to the loss of oxygen since the U_3O_8 compound becomes non-stoichiometric under atmospheric conditions at this temperature [24]. Indeed, the C_p°-temperature curve takes again, after a given temperature interval in which a partial enthalpy of vaporization of oxygen is given to the sample, a value corresponding to the extrapolation of lower temperature measurements, as shown in Fig. 10.

4.3. Thermodynamic functions

The enthalpy of formation of Holley and Hubert [75] obtained by isoperibolic calorimetry of the combustion of U into U_3O_{8-z} is retained. This value, corrected for impurities and mechanical energy, is more accurate than preceding values of Hubert et al. [76] and Popov and Ivanov [77].

The entropy of U_3O_8 is deduced from low temperature thermal capacity measurements of Westrum and Gronvold [71], including the 25.3 K transition that Oles [78] showed to be a non-magnetic one.

Among the four adiabatic calorimetric studies, Inaba et al. [72], Naito et al. [66], Girdhar and Westrum [69], Popov et al. [70] and the enthalpy increment measurements of Maglic and Herak study [68] we observe large uncertainties and some discrepancies. Popov did not observe some of the transitions, and Maglic and Herak are far below others, probably because the transitions were not occurring in the quenching process associated with drop calorimetry. Consequently we choose to fit the results of Naito et al. [66], Inaba et al. [72] and Gidhar and Westrum [69], including the low temperature data of Westrum and Gronvold [71] above 214 K. We carefully discard the C_p° peaks of the transitions (see Fig. 10) at 490 and 570 K that are treated independently, and the one at 850 K which we consider as an anomaly. The retained C_p° differs from those proposed by Cordfunke and Konings [48] and Thermodata [79] as shown in Fig. 10.

Table 10
Calorimetric techniques used in the determination of transitions in U_3O_8(s)

Authors [Ref.]	Experimental techniques	Composition O/U	Transition temperature (K)	Enthalpies (J mol^{-1})
Naito et al. [66,67]	Adiabatic calorimetry	2.663	487	213
	Electrical conductivity		573	220
	XRD	2.656	490	286
			576	266
		2.64	508	306
			562	288
			618	152
Maglic and Herak [68]	Drop calorimetry	2.667	481	271
Girdhar and Westrum [69]	Adiabatic calorimetry	2.667	482.7	171
Popov et al. [70]	Adiabatic calorimetry	2.667	$593 < T < 673$	
Westrum and Gronvold [71]	Adiabatic calorimetry	2.667	25.3	50 ($\Delta S_{tr} = 2.35$ J mol K)
Inaba et al. [72]	Adiabatic calorimetry	2.667	480	135
			570	148
			850	314

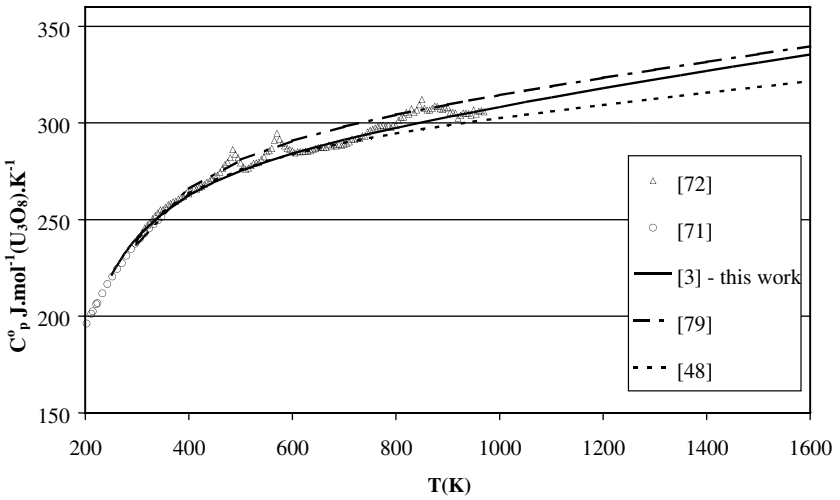

Fig. 10. Thermal capacity data of U_3O_8 from literature and comparison with proposed least square fits.

Table 11
Thermodynamic properties retained for the U_3O_8(s) compound

Property and retained value	Temperature range (K)
$\Delta H_f^\circ(298.15\ \mathrm{K}) = -3574.8 \pm 2.5\ \mathrm{kJ\,mol^{-1}}$ [75]	298.15
$S_{298}^\circ = 282.6 \pm 0.5\ \mathrm{JK^{-1}\,mol^{-1}}$ [71]	298.15
$H_{298}^\circ - H_0^\circ = 42744\ \mathrm{J\,mol^{-1}}$ [71]	0–298
$C_p^\circ = 265.42347 + 0.049381\ T - 2.99931\ 10 - 6T^2 - 3537016.4/T^2\ \mathrm{JK^{-1}\,mol^{-1}}$ [3]	298–1600
$\Delta H_{tr}^\circ = 200 \pm 70\ \mathrm{J\,mol^{-1}}$ [66,69,72]	T (transition I) $= 490 \pm 5$
$\Delta H_{tr}^\circ = 210 \pm 70\ \mathrm{J\,mol^{-1}}$ [66,67,72]	T (transition II) $= 570 \pm 5$

The thermodynamic properties selected for U_3O_8 are presented in Table 11.

5. Conclusion

The uranium oxides UO_2, U_4O_9 and U_3O_8 present some non-stoichiometric composition range that may be relatively small particularly for U_4O_9 and U_3O_8 whatever the temperature. Some transitions, mainly due to anionic and electronic rearrangements are observed, the enthalpies of which are generally quite small but which significantly affect the form of the phase diagram. The use of potentiometric methods – mainly the measurements of oxygen partial pressure – is a powerful tool in the description of these non-stoichiometric domains that was used successfully to complete usual characterization methods. This critical evaluation of the experimental data, obtained using many techniques, has allowed us to recommend a reliable set of data with a realistic set of associated uncertainties [80,81]. These two conditions are the prerequisite for a thermodynamic description of these oxides with an optimization procedure.

Addenda

During the submission of this paper, Chevalier et al. published [82] an optimization of the U–O system in which a primary data selection is made. Some references were cited that we omitted and in order to analyze their pertinence we discuss hereafter those that are really primary data determinations.

Bannister and Buykx [83] performed dilatometric measurements of the thermal expansion of UO_{2+x} samples in the range 2.01–2.20, the composition of the sample being known by emf technique referred to Markin and Bones determinations. The inflexion in the UO_{2+x} phase limit is shown to be included between 760 and 960 K, and this transition is observed to be sluggish. Data are fitted with a continuous curve, in agreement with all original data cited in this work, and with our selection of a second order transition for the U_4O_9 compound in equilibrium with the UO_{2+x} phase boundary.

Dharwadkar et al. [84] proposed an equilibrium between U_3O_{8-z} and a new compound U_8O_{21+x} from combined studies by TGA, X-ray diffraction and con-

ductivity measurements. In TGA determinations they observed 80% of non-reversibility when O_2 pressure is increased. We discussed these kinetic observations in the present paper, and discarded any data obtained under kinetic control.

Ackermann et al. [85] using thermal expansion data derived from X-ray diffraction primary data proposed for U_3O_8 a first transformation at 623 ± 10 K and a second one at 870 ± 10 K. The first one is reversible, meanwhile the second one is not. These two transition temperatures disagree with all authors cited in this paper and our retained values, or were observed with a lag time. Moreover, the oxygen potential is not always controlled and the composition of the sample may have an evolution under thermal cycling. For all these reasons, we cannot retain this work.

Enthalpies of formation for the uranium compounds that were not derived from direct calorimetric determinations – namely equilibrium data and modelling [86] were not used in our selection because these data are not primary data. Old calorimetric determinations [87] of U_3O_8 enthalpy of formation are also discarded since we cannot attribute a reasonable value for its uncertainty.

Acknowledgements

The authors acknowledge Mr G. Sauzay and COGEMA for sponsoring this study, and Dr Paul Potter for help in the preparation of the final text.

References

[1] B. Jansson, Report TRITA-MAC-0234, April 1984, Materials Center, Royal Institute of Technology, S10044 Stockholm 70, Sweden.
[2] D. Labroche, O. Dugne, C. Chatillon, Thermodynamics of the O–U system I – Oxygen chemical potential critical assessment in the UO_2–U_3O_8 composition range, J. Nucl. Mater. 312 (2003) 21.
[3] D. Labroche, Contribution à l'étude thermodynamique du système ternaire U–Fe–O, PhD at Institut National Polytechnique de Grenoble, France, 29 September 2000.
[4] F. Rossini, in: Experimental Thermochemistry, Interscience, New York, 1956, p. 308.
[5] K. Kiukkola, Acta Chem. Scand. 16 (1962) 327.
[6] T.L. Markin, R.J. Bones, UKAEA Report AERE - R4042 HL 62/2187 (C 3), 1962.
[7] Y. Saito, J. Nucl. Mater. 51 (1974) 112.
[8] D.I. Marchidan, S. Matei, Rev. Roum. Chimie 17 (1972) 1487.
[9] D.I. Marchidan, S. Matei-Tanasescu, Rev. Roum. Chimie 18 (1973) 1681.
[10] D.I. Marchidan, S. Matei-Tanasescu, Rev. Roum. Chimie 20 (1975) 1365.
[11] F. Gronvold, J. Inorg. Nucl. Chem. 1 (1955) 357.
[12] B.E. Schaner, J. Nucl. Mater. 2 (1960) 110.
[13] S. Aronson, J.E. Rulli, B.E. Schaner, J. Chem. Phys. 35 (1961) 1382.
[14] A.M. Anthony, R. Kiyoura, T. Sata, J. Nucl. Mater. 10 (1962) 8.
[15] A. Kotlar, P. Gerdanian, M. Dodé, J. Chim. Phys. 64 (1967) 862.
[16] K. Hagemark, M. Broli, J. Inorg. Nucl. Chem. 28 (1966) 2837.
[17] A. Kotlar, P. Gerdanian, M. Dodé, J. Chim. Phys. 64 (1967) 1135.
[18] A. Kotlar, P. Gerdanian, M. Dodé, J. Chim. Phys. 65 (1968) 687.
[19] P.E. Blackburn, J. Phys. Chem. 62 (1958) 897.
[20] L.E.J. Roberts, A.J. Walter, J. Inorg. Nucl. Chem. 22 (1961) 213.
[21] C. Picard, P. Gerdanian, J. Nucl. Mater. 99 (1981) 184.
[22] A. Pattoret, Etudes thermodynamiques par spectrométrie de masse sur les systèmes U–O et U–C, PhD at Université Libre de Bruxelles, Bruxelles, Belgique, 1969.
[23] R.K. Edwards, M.S. Chandrasekharaiah, P.M. Danielson, High Temp. Sci. 1 (1969) 98.
[24] R.J. Ackermann, A.T. Chang, J. Chem. Thermodyn. 5 (1973) 873.
[25] P.O. Perron, Report No. AECL-3072, 1968.
[26] P. Gerdanian, M. Dodé, Mesure directe à 1100 °C des enthalpies molaires partielles de mélanges de l'oxygène dans UO_{2+x} au voisinage de UO_2, à l'aide d'un microcalorimètre de Calvet à haute température, presented at the IAEA, Vienna, 1967, paper SM-98/5, p. 41.
[27] W. Van Lierde, J. Pelsmaekers, A. Lecocq-Robert, J. Nucl. Mater. 37 (1970) 276.
[28] R. Benz, G. Balog, B.H. Baca, High Temp. Sci. 2 (1970) 221.
[29] H. Inaba, K. Naito, J. Nucl. Mater. 49 (1973) 181.
[30] E.F. Westrum Jr., F. Gronvold, J. Am. Chem. Soc. 81 (1957) 1777.
[31] B. Belbeoch, E. Laredo, P. Perio, J. Nucl. Mater. 13 (1964) 100.
[32] T. Gilardy, Etude par analyse thermique à vitesse de transformation contrôlée des mécanismes d'oxydation et de réduction des oxydes d'Uranium, PhD Université de Provence, Aix-Marseille I, France, 1993.
[33] D.W. Osborne, E.F. Westrum, H.R. Lohr, J. Am. Chem. Soc. 79 (1957) 529.
[34] K. Naito, T. Tsuji, T. Matsui, J. Nucl. Mater. 48 (1973) 58.
[35] K. Gotoo, K. Naito, J. Phys. Chem. Solids 26 (1965) 1679.
[36] K. Seta, T. Matsui, H. Inaba, K. Naito, J. Nucl. Mater. 110 (1982) 47.
[37] J.P. Lauriat, G. Chevrier, J.X. Boucherle, J. Solid State Chem. 80 (1989) 80.
[38] H. Blank, C. Ronchi, Acta Cryst. A 24 (1968) 657.
[39] F. Gronvold, N.J. Kveseth, A. Sveen, J. Tichy, J. Chem. Thermodyn. 2 (1970) 665.
[40] T. Ishii, K. Naito, K. Oshima, Solid State Commun. 8 (1970) 677.
[41] E.F. Westrum, Y. Takahashi, F. Gronvold, J. Phys. Chem. 69 (1965) 3192.
[42] K. Naito, Solid State Commun. 5 (1967) 349.
[43] J. Tateno, J. Phys. Chem. Solids 30 (1969) 1321.
[44] A.C. McLeod, J. Chem. Thermodyn. 4 (1972) 699.

[45] B. Belbeoch, J.C. Boivineau, P. Perio, J. Phys. Chem. Solids 28 (1967) 1267.
[46] M. Dodé, B. Touzelin, Rev. Chimie Minérale 9 (1972) 139.
[47] T. Matsui, K. Naito, J. Nucl. Mater. 56 (1975) 327.
[48] E.H.P. Cordfunke, R.J.M. Konings, Thermochemical Data for Reactor Materials and Fission Products, North Holland Elsevier Science, Amsterdam, 1980.
[49] G.C. Fitzgibbon, D. Pavone, C.E. Holley, J. Chem. Eng. 12 (1967) 122.
[50] A. Burdese, F. Abbatista, Ric. Sci. 28 (1958) 1634 (cited in Ref. [48]).
[51] H.L. Glushko, L.V. Gurvich, G.A. Bergman, in: Termodinamicheskie Svoistva Individual'nykh Veshchestv IV, vol. 1, Nauka, Moscow, 1982, p. 199, vol. 2, p. 222.
[52] H.E. Flotow, D.W. Osborne, E.F. Westrum, J. Chem. Phys. 49 (1968) 2438.
[53] O. Kubachewski, C.B. Alcock, in: Metallurgical Thermochemistry, 5th Ed., Pergamon, Oxford, 1979, p. 354.
[54] I. Ansara, in: J.P. Caliste, A. Truyol, J.H. Westbrook (Eds.), Thermodynamic Modeling and Materials Data Engineering, Springer-Verlag, Berlin, 1998, p. 33.
[55] H.R. Hoekstra, S. Siegel, L.H. Fuchs, J.J. Katz, J. Phys. Chem. 59 (1955) 136.
[56] T. Sata, Bull. Tokyo Inst. Technol. 56 (1963) 21.
[57] A. Caneiro, J.P. Abriata, J. Nucl. Mater. 126 (1984) 255.
[58] T. Ishii, K. Naito, K. Oshima, J. Nucl. Mater. 36 (1970) 288.
[59] T. Matsui, T. Tsuji, K. Naito, J. Nucl. Sci. Technol. 11 (1974) 216.
[60] T. Matsui, T. Tsuji, K. Naito, J. Nucl. Sci. Technol. 11 (1974) 317.
[61] I.I. Kozhina, L.V. Shiryaeva, Radiokhimiya 16 (1974) 360.
[62] A. Caneiro, J. Nucl. Mater. 113 (1983) 260.
[63] T. Ishii, K. Naito, K. Oshima, J. Nucl. Mater. 35 (1970) 335.
[64] H. Hering, P. Pério, Bull. Soc. Chim. (France) (1952) M531.
[65] P. Pério, Bull. Soc. Chim. (France) (1953) M256.
[66] K. Naito, H. Inaba, S. Takahashi, J. Nucl. Mater. 110 (1982) 317.
[67] K. Naito, T. Tsuji, F. Ohya, J. Nucl. Mater. 114 (1983) 136.
[68] K. Maglic, R. Herak, Rev. Inter. des Hautes Tempér. Réfract. 7 (1970) 247.
[69] H.L. Gildhar, E.F. Westrum, J. Chem. Eng. Data 13 (1968) 531.
[70] M.M. Popov, Galchenko, Senin, Z. Neorg. Khim. 3 (1958) 1734.
[71] E.F. Westrum, E. Gronvold, J. Amer. Chem. Soc. 81 (1969) 777.
[72] H. Inaba, H. Shimizu, K. Naito, J. Nucl. Mater. 64 (1977) 66.
[73] A.M. George, M.D. Karhanavala, J. Phys. Chem. Solids 24 (1963) 1207.
[74] A.C. Momin, M.D. Mathews, M.D. Karkhanavala, Indian J. Chem. 9 (1971) 582.
[75] E.J. Huber, C.E. Holley, J. Chem. Thermodyn. 1 (1969) 267.
[76] E.J. Huber, C.E. Holley, E.H. Meierkord, J. Amer. Chem. Soc. 74 (1952) 3406.
[77] M.M. Popov, M.I. Ivanov, Atomnaya Energiya 2 (1957) 360 (Sov. J. Atomic Energy 2 (1957) 439).
[78] A. Oles, Nukleonika 13 (1968) 85.
[79] Thermodata Association, BP. 66, 38402 Saint Martin d'Hères, France. private communication.
[80] D. Labroche, C. Chatillon, Thermodynamics of the U–O system. Original data of the heat capacities of U_4O_9 and U_3O_8 compounds, Report CEA, DEN/DTE/STME 2001/074, 2001, France.
[81] A diskette in Excel format can be obtained from O. Dugne. e-mail: olivier.dugne@cea.fr.
[82] P.Y. Chevalier, E. Fischer, B. Cheynet, J. Nucl. Mater. 303 (2002) 1.
[83] M.J. Bannister, W.J. Buykx, J. Nucl. Mater. 55 (1974) 345.
[84] S.R. Dharwadkar, M.S. Chandrasekharaiah, M.D. Karkhanavala, J. Nucl. Mater. 71 (1978) 268.
[85] R.J. Ackermann, A.T. Chang, C.A. Sorrel, J. Inorg. Nucl. Chem. 39 (1977) 75.
[86] A. Duquesnoy, F. Marion, C.R. Acad. Sci. Paris t. 258 (1964) 4550.
[87] W.G. Mixter, Z. Anorg. Chem. 78 (1912) 221.